Title: T cell densities in brain metastases are associated with patient survival times and diffusion tensor MRI changes

Running title: MRI and immune response to brain metastases

Authors: Rasheed Zakaria[1,4], Angela Platt-Higgins[4], Nitika Rathi[2], Mark Radon[3], Sumit Das[2], Kumar Das[3], Maneesh Bhojak[3], Andrew Brodbelt[1], Emmanuel Chavredakis[1], Michael D. Jenkinson[1,5], Philip S. Rudland[4]

Affiliations 1. Department of Neurosurgery, 2. Department of Neuropathology & 3. Department of Neuroradiology, The Walton Centre NHS Foundation Trust, Liverpool, UK.

4. Institute of Integrative Biology & 5. Institute of Translational Medicine, University of Liverpool, UK

Corresponding author: Dr Rasheed Zakaria PhD, Neuroscience Research Office, The Walton Centre NHS Foundation Trust, Lower Lane, Fazakerley, Liverpool, L9 7LJ, UK. Tel: 0151 525 3611 Email: rzakaria@nhs.net

Financial support: The authors declare no competing financial interests. R. Zakaria received support from The Medical Research Council (MRC) UK - grant MR/L017342/1 and the Royal College of Surgeons of England (RCS) via a Research Training Fellowship. P.S. Rudland received support from the Cancer and Polio Research Fund, UK and MRC (UK) - grant G0801447.

Abstract

Brain metastases are common and are usually detected by magnetic resonance imaging (MRI). Diffusion tensor imaging (DTI) is a derivative MRI technique which can detect disruption of white matter tracts in the brain. We have matched preoperative DTI with image-guided sampling of the brain-tumor interface in 26 patients during resection of a brain metastasis and assessed mean diffusivity (MD) and fractional anisotropy (FA). The tissue samples were analysed for vascularity, inflammatory cell infiltration, growth pattern, and tumor expression of proteins associated with growth or local invasion such as Ki67, S100A4, and MMP2, 9, and 13. A lower FA in the peritumoral region indicated more white matter tract disruption and independently predicted longer overall survival times (HR for death = 0.21, 95% CI 0.06 - 0.82, p=0.024). Of all the biological markers studied, only increased density of CD3+ lymphocytes in the same region correlated with decreased FA (Mann Whitney U, p=0.037) as well as confounding completely the effect of FA in multivariate survival analyses. We conclude that the T cell response to brain metastases is not a surrogate of local tumor invasion, primary cancer type, or aggressive phenotype and is associated with patient survival time regardless of these biological factors. Furthermore, it can be assayed by DTI, potentially offering a quick, non-invasive, clinically available method to detect an active immune microenvironment and, in principle, to measure susceptibility to immunotherapy.

Introduction

Brain metastases (BM) are a profound clinical problem, causing significant morbidity and mortality in patients with solid organ cancers, however they are poorly responsive to traditional chemotherapeutic agents. There has been little investigation of the interface between the brain and the brain metastasis (B-BM) in patients undergoing treatment, however there are now strong reasons for doing so (1-3). First, it has recently been shown that far from being discrete and encapsulated, brain metastases show a variety of growth patterns at the leading edge, with implications for prognosis and treatment (1,4). Second, the B-BM interface is the region in which the tumor interacts with the host immune system (5,6). Third, there are new treatments which act at the B-BM interface: cavity boost radiosurgery in radiation oncology, immune modulating agents in medical oncology and supra-marginal resection in neurosurgery (7,8).

MRI provides a quick, widely available modality to assess the B-BM interface non-invasively, and can deliver information that applies to both resected and non-resected tumors. Diffusion along white matter tracts in the brain assessed by MRI is particularly sensitive at detecting changes at the B-BM interface (9,10) although MR spectroscopy (for tumour metabolism, cellular proliferation) and MR perfusion (for increased blood flow) may also detect changes not seen on conventional imaging. Disruption of white matter tracts causes reduced fractional anisotropy (FA) without necessarily reducing mean diffusivity (MD) and this may indicate local tumor invasion - as has been demonstrated by meta-analysis in glioma (11,12) - and/or other processes, such as inflammation or neoangiogenesis. Diffusion MRI has the further advantage

of being quick to obtain, relatively easy to post process and reproducible across different scanners or institutions(13).

We have performed matched diffusion MRI (measuring FA & MD) with image-guided sampling of the B-BM interface for newly diagnosed patients undergoing surgery to assess MRI features, cellularity, growth pattern, cell invasion/division and host inflammatory responses for brain metastases from different primary cancers in an attempt to relate them to the MRI data and patient outcomes.

Material & Methods

Patients & follow up

Overall 26 patients were studied prospectively and the clinical details are summarised in **Table 1**. Patient study was conducted in accordance with the principles of the Declaration of Helsinki. Ethical approval was granted as an internal project within the institution's Research Tissue Bank after board review (National Research Ethics Service ID 11/WNo03/2) and patients provided written, informed consent for inclusion in this bank before surgery. All patients underwent complete resection of a symptomatic, supratentorial BM in the course of routine clinical care (including dexamethasone 16mg per day in divided doses for at least 72 hours prior to surgery) at a single institution. Post-operative clinical course and care including radiotherapy or the use of adjuvant systemic chemotherapy (including targeted agents) were recorded prospectively, as

these were potential confounding factors for survival. Intracranial progression was determined by a neuro-radiologist as per standard criteria (14) in combination with the clinical findings, and all patients were discussed at the interdisciplinary tumor board.

MRI studies and image guided sampling

At a median of 5 days prior to surgery, patients underwent an MRI brain scan protocoled by a clinical neuro-radiologist, further details of sequences are provided in *Supplementary Methods* but are summarised here. A volumetric fast spoiled gradient echo sequence was taken after gadolinium injection at a standard dose of 0.1mmol/kg (repetition time/echo time 9/1.4ms, flip angle 15 degrees, acquisition matrix 256×256, volume 180 × 1 mm^2 slices at zero angle gantry); this is referred to as the planning scan. Scans were reviewed by a clinical neuro-radiologist including scoring the degree of edema on T2 weighted using a previously defined scale (15). Following standard post-processing (e.g. to correct for eddy current distortion) maps of fractional anisotropy (FA) and mean diffusivity (MD) were generated using DTIstudio, version 3.0.3(16). In theatre the planning scan was used for registration to a neuro-navigation system (StealthStation S7, Medtronic Inc., MN, USA). For each case a biopsy location was chosen which showed a radiological and histological interface with brain. In the course of tumor resection, patients had image guided samples taken from this location using standard forceps with a tracking device attached, so that the realtime location of the forceps tip could be followed. These forceps yielded specimens of approximately 4x 3x 2mm^3 and the location was electronically marked on the planning scan as samples were taken (17).

After surgery, the vector specifying this location was extracted from the image guidance software and transferred offline to the image analysis software. Each location was double checked visually with screenshots taken in three orthogonal planes at the biopsy location during surgery. A region of interest (ROI) placed at this location in the image analysis software, which was co-localised to the tissue sample taken intra-operatively, could then be applied to the MRI parametric maps generated as these maps were also co-registered to the planning scan. Average and minimum readings of MD and FA were taken on the tumor and brain side of the B-BM interface at the biopsy location for each case**.** Control readings were taken from the contralateral white matter by flipping the ROIs across the anatomical midline, ensuring that this avoided any confounding structures such as ventricles or bone.

Tissue analysis

Histological assessment by a neuropathologist was performed to determine the primary cancer of origin, confirm the diagnosis of metastasis and categorise the growth pattern (4). A number of proteins acting as markers of proliferation (Ki67), glial cells (GFAP), inflammatory cells (CD3, CD8, CD4, CD20, CD68, FOXP3, PD1), connective tissue (reticulin, CD34), ECM adhesion/remodelling (MMP 2,9,13) and metastasis (S100A4, S100P, AGR2, OPN) were examined by immunohistochemistry and manually and electronically scored for how intense and widespread the staining was using validated methods (18). Absolute numbers of immunoreactive lymphocytes and macrophages were manually counted per high powered field; further detail on the methods as well as how biopsy samples were processed and the

types and serial numbers of commercially available antibodies are provided online in *Supplementary Methods*.

Statistical methods

Overall survival (OS) was taken as the time from surgery to death; a non-cancer death or those lost to follow up were censored at the last recorded follow up. Patients who died before progression were censored at the last date of follow up imaging. Significant differences were assessed using Fisher's Two-sided Exact Test. Time-to-event comparisons were made using the Kaplan-Meier method with Log Rank tests and multivariate analyses conducted using Cox's method. Correlations were assessed using Spearman's Rank Test and pairwise comparisons using Wilcoxon's Signed Rank Test. Data processing was performed using SPSS version 22.0 (IBM, Chicago, IL) and R version 3.10 (R Core Team, 2013).

Results

Clinical outcomes

Post-operative CT brain scan within 24 hours confirmed complete resection of the contrast-enhancing lesion and there were no post-operative complications such as infection or haematoma. Median overall survival (OS) was 5.5 months (95% CI 4.2 – 6.8). The only factors associated with increased OS were tumor size (median 8.2 months < 30mm diameter vs. 5.2 months if larger, Log Rank 5.65, p=0.017) and administration of postoperative whole brain

radiotherapy (WBRT) (median 6.5 months versus 2.7 months untreated, Log Rank 16.26, $p<0.001$).

MRI suggests two different prognostic phenotypes, unrelated to biological features of the tumor

The median fractional anisotropy (FA) readings in the peritumoral region where tissue was obtained from were consistently lower than control white matter from the comparable brain region in the unaffected, contralateral hemisphere (0.140, interquartile range (IQR) 0.106 – 0.176, versus 0.198, IQR 0.162 – 0.235, matched samples Wilcoxon-signed Rank Test, $p<0.001$). We observed two populations within the group, as illustrated in **Figure 1A - F**. Those cases with a low peritumoral FA (<median), showed significantly longer survival times (median 9.9 months, 95% CI: 7.4-12.4 versus 5.3 months, 95% CI: 3.4 – 7.13, Log Rank = 4.57, $p=0.033$), **Figure 1G & H**, even when confounding variables were introduced (Cox's multivariate analysis: **Table 2A & B**; HR for death = 0.21, 95% CI 0.06 – 0.82, $p=0.024$). The co-localised samples obtained at the B-BM interface were analysed in relation to the different MRI phenotypes (high FA vs. low FA). The primary cancer type and metastasis growth pattern (diffuse versus encapsulated) as assessed by a neuropathologist (4) did not show any association with FA readings at the leading edge of the tumor or in the adjacent peritumoral region. There was no difference in the tumor expression of relevant matrix-metalloproteinases (MMP 2, 9 & 13), tumor cellularity, Ki67 proliferative index, tumor or peritumoral vascularity (assessed as CD34 positive blood vessel density), necrosis or connective tissue density (reticulin and GFAP staining) between the high and low FA cases.

Local cellular immune response is heterogeneous and unrelated to biological features of the tumor

Assessment of the cellular immune response at the B-BM interface revealed a dense CD68-positive macrophage infiltration compared to the metastasis core - median 62 cells per high powered field (HPF), IQR 43-105 in peritumoral regions versus 21 cells/HPF (IQR 13-33) in control white matter; these cells formed a band surrounding the tumor rather than focal islands or a diffuse infiltrate extending away from the tumor edge. In contrast, T-cell (CD3-positive lymphocyte) infiltration was heterogeneous (**Figure 1B,E,C,F & Figure 2A**). Although consistently present in the peritumoral region (median 16 cells/HPF, significantly greater than control white matter, Mann-Whitney U, $p<0.001$), the density of T-cells varied from 0 to 113 cells / HPF. This was not a function of the primary cancer type nor of any clinical features tested, e.g. control of the primary cancer, presence of extracranial metastases, intra-cranial location, growth pattern, markers of aggressive growth/invasion or patient age (all comparisons non-significant by Kruskal-Wallis test). Low B-cell (CD20-positive) infiltration was observed in all regions (**Figure 2A**).

Peritumoral T- cell infiltrates were further stained for CD4, CD8, FOX-P3 and PD-1 **(Figure 2B)**. Mean ratio of cytotoxic (CD8+) to helper (CD4+) cells in the peritumoral region was 1.5:1, with no significant difference observed by primary cancer or any other biological factor relating to the metastasis or the patient (Kruskal-Wallis & Friedman's Analysis of Variance by Ranks tests). The percentage of regulatory, FOX-P3 positive T cells varied from 34% in the core to 24% at the

leading edge and 16% in the peritumoral region, with a lower density of FOX-P3 positive cells in those brain metastases with extracranial metastases (Mann-Witney U, p=0.001) and those presenting with a previously-treated primary cancer (Mann-Witney U, p=0.012). Regarding possible susceptibility to existing immunotherapy drugs, 52% of T-cells in the peritumoral region were PD-1 receptor positive (compared to 15% in core and 25% at leading edge) and the proportion of T-cells that were PD-1 positive was no greater around or in those BMs expressing PD-L1. PD-L1 staining was detected in 13/26 tumors studied with no relation to the primary cancer nor the levels of immune cells seen and no effect on patient survival in this series.

Peritumoral T cells are associated with low FA and prolonged patient survival

The peritumoral density of CD3+ T-cells was the only significant biological difference observed between the high and low FA groups (Mann-Whitney U, p=0.037); there were no differences in the presence of other immunoreactive cells in the same region (macrophages p=0.867, B-cells p=0.074, all immune cells combined p=0.232) nor in vascularity (CD34+ blood vessels p=0.673). The continuous values for peritumoral T-cell density and peritumoral FA were compared to matched samples and these correlated strongly (Spearman's rho = -0.676, p=0.003), whereas there was no significant correlation with other MRI features such as the degree of T2 oedema (0.233, p=0.262). There was no difference in the mean diffusivity (MD) in those cases with high versus low peritumoral T-cell infiltration (median samples test p=0.684) and no correlation of the MD with T-cell density (Spearman 0.113, p=0.599).

The differential response in different brain metastases is clinically relevant, since increased peritumoral CD3+ T-cell density was significantly associated with prolonged survival time (median 8.1 months vs. 5.2 months, Log Rank 5.77, p=0.016; **Figure 2C**, **Table 2B-D**). When further categorised into 3 groups (<5, 5-25 and >25 immunoreactive cells per high power field), those patients with moderate peritumoral CD3+ T-cell infiltration appeared to be at no advantage compared to those with low infiltration, whereas those with the highest infiltration lived over twice as long (median 11.7 months vs. 5.1, 5.2 months for moderate and low groups respectively, Log Rank (pooled) =10.06, 2 d.f., p=0.007) (**Figure 1G, Figure 2D**). A number of important biological factors were excluded as potential confounders including macrophage, B-cell, T-cell subtypes (CD4/8/FOX-P3/PD-1), growth pattern (invasive or pseudo-encapsulated), metalloproteinases (MMP 2, 9, 13) or metastasis-inducing proteins (19), cellularity, Ki67 proliferative index, vascularity, necrosis, connective tissue density at the leading edge and clinical factors, such as extracranial metastases, primary cancer, age and performance status. However, when both low FA and high peritumoral levels of T-cells were included in Cox's multivariate analysis either alone (**Table 2A & B**) or with the other potentially confounding variables (**Table 2D**), high peritumoral T cell density completely confounds low peritumoral FA in its association with patient survival times so rendering the contribution from FA completely insignificant **(Table 2C)**. This result suggests that both are a reflection of the same or associated phenomenon irrespective of the other variables.

Discussion

Since the nature of samples obtained in this study are not routinely available in clinical practice unless intentionally performing a supramarginal resection (7,8), this is the first *in vivo* examination of the relationship between white matter disruption and inflammation for BMs. Here, we have shown for the first time that the FA in the peritumoral region is closely associated with the density of CD3+ T-cell infiltration but the MD is not. Both increased T-cell infiltration and reduced FA (corresponding to more white matter tract disruption) are associated with prolonged overall survival time after resection of the metastasis, and one parameter completely confounds the other in this respect. Since all the imaging and biological data are obtained from the same region using image guided surgical procedures, we suggest that FA in the peritumoral region is possibly acting as a surrogate marker of the immune response to the BM. This is a novel finding which further supports the existing evidence for the tumor microenvironment in mediating BM behaviour and adds the possibility of assaying this inflammatory response non-invasively in patients with different primary cancers, in a clinically relevant context, using a widely available and studied imaging technique.

The MRI characteristics of BMs have been extensively studied previously using DWI and DTI and readings obtained in our series are entirely in keeping with those previously recorded, although not their interpretation. Even those studies which focused on the B-BM interface by measuring changes in the peritumoral region have focused exclusively on invasion (11,12). However, the brain is uniquely sensitive to inflammatory changes and hence white matter disruption, assessed by changes in anisotropic diffusion, have been shown in a variety of pathologies in

large numbers (20). In contrast to glioma, brain metastases do not diffusely infiltrate the brain, therefore the change in white matter signal may have a different cause than simple invasion. Since the CNS is an immune privileged environment, the DTI changes may be inflammatory, as suggested by post mortem (21), animal (10) and now *in vivo* human study.

Our patient group is not unusual except that traditional predictive factors such as age and performance status - which are incorporated in scoring systems (22) - were not significant for survival. However, all the patients selected for neurosurgical intervention would tend to be of high performance status and younger age in any case, explaining this finding. The image guidance system used is of the sort routinely used in clinical neurosurgical practice in Europe and North America and localisation accuracy is dependent on a number of factors from the fidelity of the planning MRI to the image registration algorithms. Accuracy could potentially be improved by using rigid frame based neuro-navigation or a robot mounted tool to take samples as opposed to a hand held forceps, but this would limit the angle of sampling and ability to manoeuvre the probe to the true B-BM interface under direct vision and navigation. Finally, in neuro-navigation there is an issue of brain shift where the pre-registered navigation loses some accuracy once the dura is opened and CSF is released. Although this can be corrected for potential inaccuracy using intraoperative ultrasound, this procedure is not routine clinical practice as it requires intense computational power and incurs a time delay, for little benefit in accuracy when dealing with mostly superficial tumors (metastases are usually seen at the grey-

white matter zone), where underlying brain edema often balances the loss of CSF on opening the dura.

Immune response and in particular quantifying tumor-associated CD3+ T-cells is currently of great interest as a means of improving prognostication and developing therapies in cancer medicine. A small number of descriptions have disagreed on the *degree* of T cell infiltration in brain metastases from solid organ cancers (5,23). Here we show there is considerable variation in inflammatory cells with location, and this does not depend on the primary tumor type or the growth pattern of the BM; this is important in studying the biology of these tumors, given recent study has suggested that there may be more and less locally invasive subtypes(1). Furthermore proteins known to be involved in local invasion and recently found to be highly associated with local recurrence and overexpressed at the BM leading edge (19) do not appear to modulate the local cellular immune response, nor did the BM expression of PD-L1. The latter result suggests more caution is needed if PD-L1 expression is to be taken as the sole marker of susceptibility to immune modulating therapies in some primary types (e.g. melanoma)(5).

There is an urgent need for better biomarkers of susceptibility to immunotherapy. These treatments, although potentially huge in their impact on survival for patients with metastatic disease, are only effective in some cases (perhaps 20-50% depending on estimates) and they have considerable costs, both financial and in terms of potentially harmful side effects. There remains no standard criteria for predicting tumor response and responses are difficult to distinguish during tumor growth using conventional imaging although reports using other

modalities are emerging(24). Diffusion MRI is a well-established technique with huge numbers of reports on the theoretical basis and practical application in neuro-oncology imaging. It is therefore highly important if this technique could be re-purposed to predict in advance of obtaining tissue (often not performed for brain metastases patients with an established primary cancer) whether there is an “immune active” microenvironment in this case T-cell infiltration, which is known to be a predictor of response to immunotherapy(25). Further longitudinal study with imaging at multiple time points or after immunotherapy would be important in validating this finding although repeat, corroborative tissue sampling from peritumoral brain is unlikely to be obtained in the future.

In conclusion we have tested and excluded the hypothesis that the immune reaction to brain metastases depends on tumor factors such as primary cancer type, growth pattern and expression of proteins mediating local invasion and recurrence. We have shown instead that the CD3+ T-cell density in the peritumoral region is the only biological factor independently associated with overall survival for patients with an operated brain metastasis from solid organ cancers. Higher T-cell infiltration in this region co-localises with white matter disruption and a decrease in anisotropic diffusion as measured non-invasively by DTI. Since the immune response is a marker of susceptibility to immune modifying drugs and most patients with brain metastases are not suitable for resection and hence tissue biomarkers, this is therefore a routinely available clinical technique that could in future be used as part of the work up before considering immunotherapy.

Acknowledgments: We thank Mr Khaja Syed of The Walton Centre NHS Foundation Trust for his assistance with tissue banking. This work has been presented at the EORTC Brainmets conference 2016 and the AACR Tumor Immunotherapy and Immunology Meeting 2016, being published as an abstract in the proceedings of those meetings.

References

1. Siam L, Bleckmann A, Chaung HN, Mohr A, Klemm F, Barrantes-Freer A*, et al.* The metastatic infiltration at the metastasis/brain parenchyma-interface is very heterogeneous and has a significant impact on survival in a prospective study. Oncotarget **2015**;6(30):29254-67 doi 10.18632/oncotarget.4201.
2. Raore B, Schniederjan M, Prabhu R, Brat DJ, Shu HK, Olson JJ. Metastasis infiltration: an investigation of the postoperative brain-tumor interface. International journal of radiation oncology, biology, physics **2011**;81(4):1075-80 doi 10.1016/j.ijrobp.2010.07.034.
3. Baumert BG, Rutten I, Dehing-Oberije C, Twijnstra A, Dirx MJ, Debougnoux-Huppertz RM*, et al.* A pathology-based substrate for target definition in radiosurgery of brain metastases. International journal of radiation oncology, biology, physics **2006**;66(1):187-94 doi 10.1016/j.ijrobp.2006.03.050.
4. Berghoff AS, Rajky O, Winkler F, Bartsch R, Furtner J, Hainfellner JA*, et al.* Invasion patterns in brain metastases of solid cancers. Neuro-oncology **2013**;15(12):1664-72 doi 10.1093/neuonc/not112.
5. Kluger HM, Zito CR, Barr ML, Baine MK, Chiang VL, Sznol M*, et al.* Characterization of PD-L1 expression and associated T-cell infiltrates in metastatic melanoma samples from variable anatomic sites. Clinical cancer research : an official journal of the American Association for Cancer Research **2015**;21(13):3052-60 doi 10.1158/1078-0432.ccr-14-3073.
6. Sugihara AQ, Rolle CE, Lesniak MS. Regulatory T cells actively infiltrate metastatic brain tumors. International journal of oncology **2009**;34(6):1533-40.
7. Yoo H, Kim YZ, Nam BH, Shin SH, Yang HS, Lee JS*, et al.* Reduced local recurrence of a single brain metastasis through microscopic total resection. Journal of neurosurgery **2009**;110(4):730-6 doi 10.3171/2008.8.JNS08448.
8. Kamp MA, Rapp M, Slotty PJ, Turowski B, Sadat H, Smuga M*, et al.* Incidence of local in-brain progression after supramarginal resection of cerebral metastases. Acta neurochirurgica **2015**;157(6):905-10; discussion 10-1 doi 10.1007/s00701-015-2405-9.
9. Zakaria R, Das K, Radon M, Bhojak M, Rudland PR, Sluming V*, et al.* Diffusion-weighted MRI characteristics of the cerebral metastasis to brain boundary predicts patient outcomes. BMC medical imaging **2014**;14:26 doi 10.1186/1471-2342-14-26.
10. Serres S, Martin CJ, Sarmiento Soto M, Bristow C, O'Brien ER, Connell JJ*, et al.* Structural and functional effects of metastases in rat brain determined by multimodal MRI. International journal of cancer Journal international du cancer **2014**;134(4):885-96 doi 10.1002/ijc.28406.
11. Lemercier P, Paz Maya S, Patrie JT, Flors L, Leiva-Salinas C. Gradient of apparent diffusion coefficient values in peritumoral edema helps in differentiation of glioblastoma from solitary metastatic lesions. AJR American journal of roentgenology **2014**;203(1):163-9 doi 10.2214/ajr.13.11186.
12. Jiang R, Du FZ, He C, Gu M, Ke ZW, Li JH. The value of diffusion tensor imaging in differentiating high-grade gliomas from brain metastases: a systematic review and meta-analysis. PloS one **2014**;9(11):e112550 doi 10.1371/journal.pone.0112550.
13. Grech-Sollars M, Hales PW, Miyazaki K, Raschke F, Rodriguez D, Wilson M*, et al.* Multi-centre reproducibility of diffusion MRI parameters for clinical sequences in the brain. NMR in biomedicine **2015**;28(4):468-85 doi 10.1002/nbm.3269.
14. Lin NU, Lee EQ, Aoyama H, Barani IJ, Barboriak DP, Baumert BG*, et al.* Response assessment criteria for brain metastases: proposal from the RANO group. The Lancet Oncology **2015**;16(6):e270-8 doi 10.1016/s1470-2045(15)70057-4.

15. Spanberger T, Berghoff AS, Dinhof C, Ilhan-Mutlu A, Magerle M, Hutterer M*, et al.* Extent of peritumoral brain edema correlates with prognosis, tumoral growth pattern, HIF1a expression and angiogenic activity in patients with single brain metastases. Clinical & experimental metastasis **2013**;30(4):357-68 doi 10.1007/s10585-012-9542-9.
16. Jiang H, van Zijl PC, Kim J, Pearlson GD, Mori S. DtiStudio: resource program for diffusion tensor computation and fiber bundle tracking. Comput Methods Programs Biomed **2006**;81(2):106-16 doi 10.1016/j.cmpb.2005.08.004.
17. Zakaria R, Jenkinson MD. Using ADC maps with structural scans to improve intraoperative biopsy specimens in brain metastases. The neuroradiology journal **2014**;27(4):422-4 doi 10.15274/nrj-2014-10075.
18. Rudland PS, Platt-Higgins A, Renshaw C, West CR, Winstanley JH, Robertson L*, et al.* Prognostic significance of the metastasis-inducing protein S100A4 (p9Ka) in human breast cancer. Cancer research **2000**;60(6):1595-603.
19. Zakaria R, Platt-Higgins A, Rathi N, Crooks D, Brodbelt A, Chavredakis E*, et al.* Metastasis-inducing proteins are widely expressed in human brain metastases and associated with intracranial progression and radiation response. British journal of cancer **2016**;114(10):1101-8 doi 10.1038/bjc.2016.103.
20. Jiang Q, Zhang ZG, Chopp M. MRI evaluation of white matter recovery after brain injury. Stroke; a journal of cerebral circulation **2010**;41(10 Suppl):S112-3 doi 10.1161/strokeaha.110.595629.
21. Berghoff AS, Lassmann H, Preusser M, Hoftberger R. Characterization of the inflammatory response to solid cancer metastases in the human brain. Clinical & experimental metastasis **2013**;30(1):69-81 doi 10.1007/s10585-012-9510-4.
22. Sperduto PW, Kased N, Roberge D, Xu Z, Shanley R, Luo X*, et al.* Summary report on the graded prognostic assessment: an accurate and facile diagnosis-specific tool to estimate survival for patients with brain metastases. Journal of clinical oncology : official journal of the American Society of Clinical Oncology **2012**;30 doi 10.1200/jco.2011.38.0527.
23. Berghoff AS, Ricken G, Widhalm G, Rajky O, Dieckmann K, Birner P*, et al.* Tumour-infiltrating lymphocytes and expression of programmed death ligand 1 (PD-L1) in melanoma brain metastases. Histopathology **2015**;66(2):289-99 doi 10.1111/his.12537.
24. Larimer BM, Wehrenberg-Klee E, Caraballo A, Mahmood U. Quantitative CD3 PET Imaging Predicts Tumor Growth Response to Anti-CTLA-4 Therapy. Journal of nuclear medicine : official publication, Society of Nuclear Medicine **2016**;57(10):1607-11 doi 10.2967/jnumed.116.173930.
25. Gnjatic S, Bronte V, Brunet LR, Butler MO, Disis ML, Galon J*, et al.* Identifying baseline immune-related biomarkers to predict clinical outcome of immunotherapy. Journal for immunotherapy of cancer **2017**;5:44 doi 10.1186/s40425-017-0243-4.

Table 1: Clinical features of patients studied.

Characteristic		Number	% of total
Age at surgery / years (range)		62.9	(23.8 – 76.0)
Gender	Female	14	53.8%
	Male	12	46.2%
Karnofsky performance score	80	5	19.2%
	90	18	69.2%
	100	3	11.5%
Primary cancer	Non-small cell lung	13	50%
	Breast	4	15.4%
	Melanoma	4	15.4%
	Colorectal	2	7.7%
	Renal	1	3.8%
	Other	2	7.7%
Extra-cranial metastases	Absent	18	69.2%
	Present	8	30.8%
Control of primary disease	Synchronous	9	34.6%
	Controlled	17	65.4%
Adjuvant WBRT* (30Gy in 10#)	No	5	19.2%
	Yes	21	80.8%
Adjuvant chemotherapy	None	13	50.0%
	Yes	9	34.6%
	Targeted agent	4	15.4%
Overall Survival /months (range)		5.8	(1.6 – 15.5)
Intracranial progression	None	16	61.5%
	Local	7	26.9%
	Distant	3	11.5%
Progression free survival /months(range)		3.8	(0.2 – 12.9)

*WBRT = whole brain radiotherapy

Table 2: Multivariate Cox proportional hazards model for overall survival. Models incorporating: A. All factors that were significant at univariate Log Rank analysis. B. All factors significant at univariate analysis but with T cell density substituted for peritumoral fractional anisotropy (FA). C. Only FA and peritumoral T-cell infiltration, which confound one another. D. All factors significant at univariate analysis including both FA and peritumoral T-cell density.

A	**HR for death**	**95% CI for HR**	**Sig.**
Adjuvant whole brain radiotherapy given	0.08	0.01 – 0.51	0.008*
Tumor size: longest axis > 30mm	2.80	0.85 – 9.25	0.091
Low peritumoral FA (more white matter tract disruption)	0.21	0.06 – 0.82	0.024*
B	**HR for death**	**95% CI for HR**	**Sig.**
Adjuvant whole brain radiotherapy given	0.10	0.03 – 0.39	0.001*
Tumor size: longest axis > 30mm	3.37	1.29 – 8.81	0.013*
High peritumoral density of CD3+ T-cells	0.40	0.13 – 1.25	0.114
C	**HR for death**	**95% CI for HR**	**Sig.**
Low peritumoral FA (more white matter tract disruption)	0.96	0.26 – 4.19	0.964
High peritumoral density of CD3+ T-cells	0.08	0.12 – 0.49	0.007*
D	**HR for death**	**95% CI for HR**	**Sig.**
Adjuvant whole brain radiotherapy given	0.29	0.04 – 2.33	0.242
Tumor size: longest axis > 30mm	3.11	0.87 – 11.18	0.082
High peritumoral density of CD3+ T-cells	0.09	0.01 – 1.13	0.062
Low peritumoral FA (more white matter tract disruption)	0.83	0.11 – 6.58	0.862

Figure 1: Two different populations of brain metastases identified by diffusion tensor imaging (DTI). A. lung adenocarcinoma metastasis which shows little white matter disruption and has a high peritumoral fractional anisotropy (FA) value at the biopsy location shown; B. H&E of biopsy; C. CD3 stained serial section showing sparse T cell infiltration in the same region (inset magnified). D. In contrast, a breast cancer metastasis shows more visible white matter change and the FA value in the peritumoral region shown is lower. E. H&E, F. CD3 stained section of biopsy. Here, there is dense peritumoral T cell infiltration (inset, magnified). G. Values of FA differentiated categories of peritumoral CD3+ T-cell density in the co-localised image-guided biopsy regions, the differences are significant (Kruskal-Wallis, $p=0.033$). H. Cases with high peritumoral FA (>median) died significantly sooner after neurosurgical resection of their metastasis than those with a low peritumoral FA (9.9 months vs. 5.3 months, log rank statistic = 4.566, $p=0.033$).

Figure 2: Cellular immune reaction to brain metastases. Absolute numbers of immunoreactive cells per high powered field (cells/HPF) were counted in specimens obtained from image-guided resection of brain metastases. A. Highest infiltrates were present in the peritumoral region for both CD68+ macrophages (median 62 cells/HPF, 95% CI 45 – 105) and CD3+ T-cells (median 16 cells/HPF, 95% CI 6 – 25) whilst few or no CD20+ B cells were seen (median 0 cells/HPF, 95% CI 0.1 – 1.1). B. T-cells seen were a mixture of CD8+ effector cells and CD4+ helper cells, with PD-1 receptor positive and regulatory FOX-P3 positive cells occurring predominantly at the tumor edge and peritumoral region. C. High peritumoral T-cell count (>16 cells per PHF) was associated with improved overall survival times for resected brain metastases, compared to lower than median count (<16 cells per HPF) (log rank test = 5.77, p = 0.016). D. Highest peritumoral T-cell counts (>25 per HPF) were associated with longer overall survival times compared to moderate (5-25) and low (<5) T-cell counts (Log Rank statistics = 10.15, 4.84 and p = 0.001, 0.028 respectively). There was no significant difference between moderate and low T-cell counts (Log Rank 0.242, p=0.623).

Figure 1

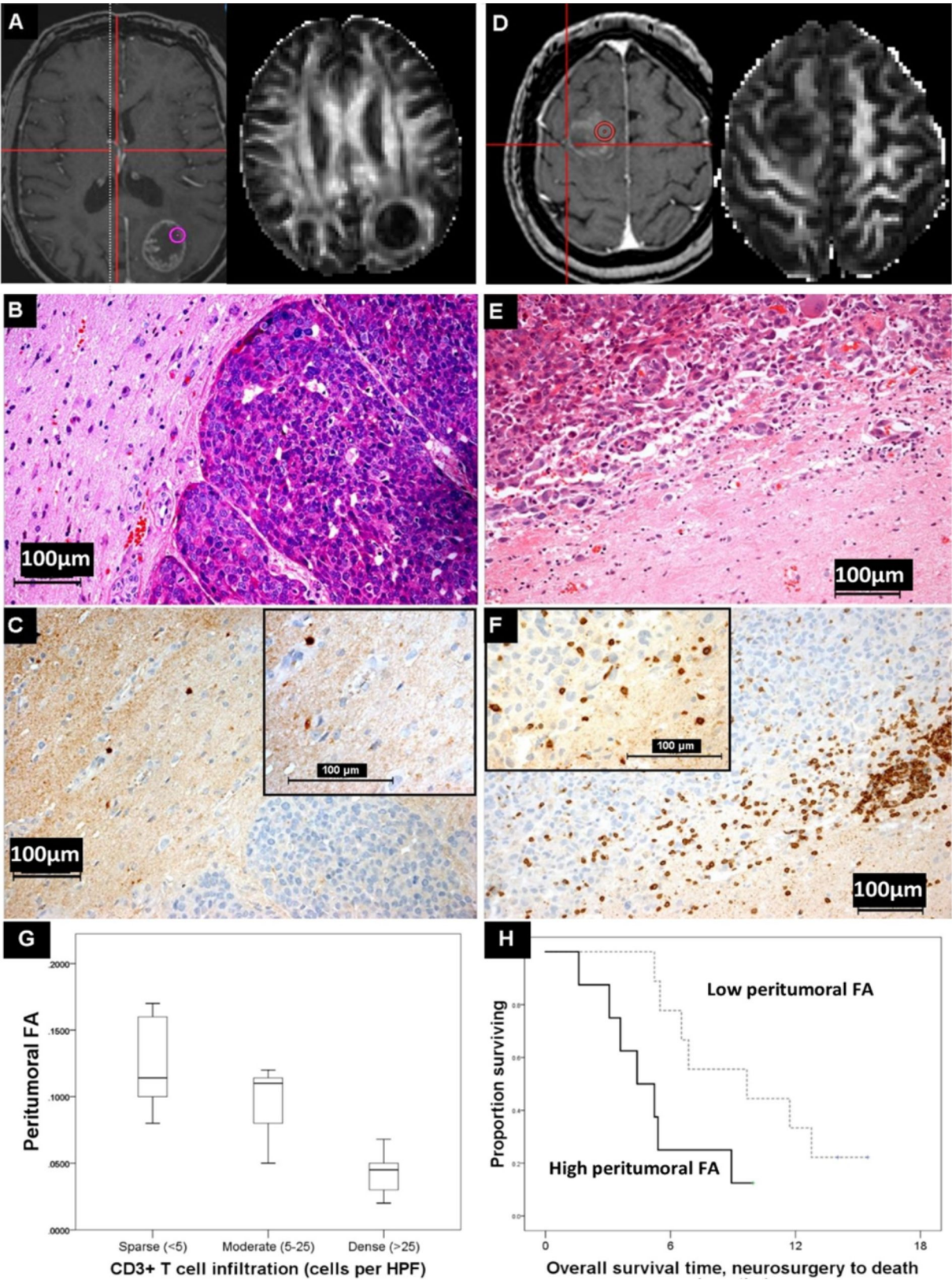
A
D
B
100µm
E
100µm
C
100 µm
100µm
F
100 µm
100µm
G
Peritumoral FA
.2000
.1500
.1000
.0500
.0000
Sparse (<5)
Moderate (5-25)
Dense (>25)
CD3+ T cell infiltration (cells per HPF)
H
Low peritumoral FA
High peritumoral FA
Proportion surviving
0
6
12
18
Overall survival time, neurosurgery to death

Figure 2

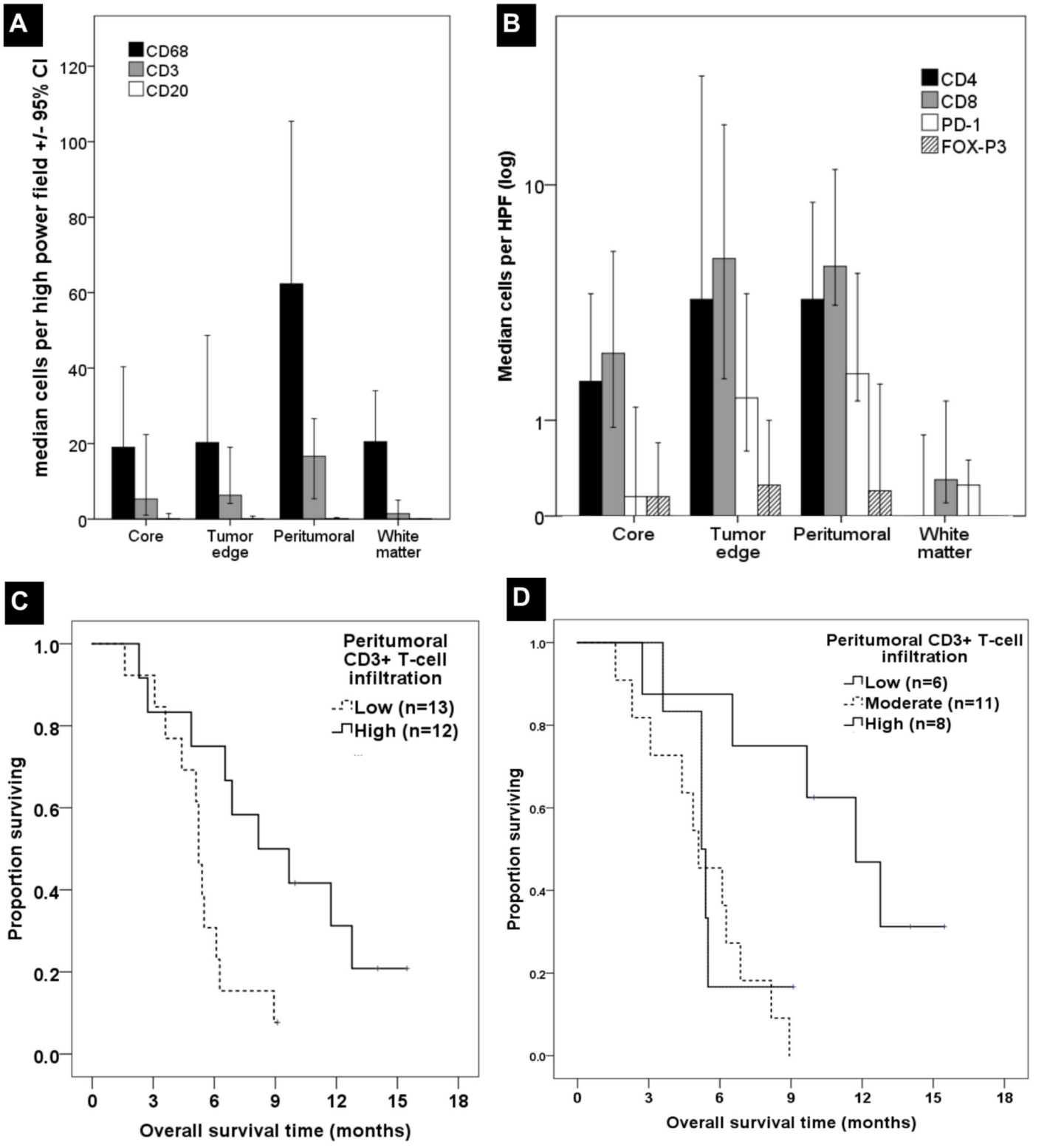
A
CD68
CD3
CD20
median cells per high power field +/- 95% CI
120
100
80
60
40
20
0
Core
Tumor edge
Peritumoral
White matter
B
CD4
CD8
PD-1
FOX-P3
Median cells per HPF (log)
10
1
0
Core
Tumor edge
Peritumoral
White matter
C
Peritumoral CD3+ T-cell infiltration
Low (n=13)
High (n=12)
Proportion surviving
1.0
0.8
0.6
0.4
0.2
0.0
0
3
6
9
12
15
18
Overall survival time (months)
D
Peritumoral CD3+ T-cell infiltration
Low (n=6)
Moderate (n=11)
High (n=8)
Proportion surviving
1.0
0.8
0.6
0.4
0.2
0.0
0
3
6
9
12
15
18
Overall survival time (months)